ORIGINAL PAPER

# A comprehensive study of Cd(II) ions removal utilizing high-surface-area binary Mg–Si hybrid oxide adsorbent

F. Ciesielczyk[1] · P. Bartczak[1] · T. Jesionowski[1]

**Abstract** Presented work concerns the application of synthetic oxide adsorbent in the removal of cadmium ions from its model, water solutions. In this study, a novel magnesium–silicon (Mg–Si) binary oxide adsorbent was prepared by a modified co-precipitation method, utilizing sodium silicate and magnesium sulphate solutions as precursors of silica and magnesium oxide, respectively. The material was thoroughly characterized in order to evaluate chemical composition (AAS, EDS and gravimetric method), crystalline structure (XRD), morphology (SEM), particle size distribution (DLS), characteristic functional groups (FTIR) and porous structure parameters (BET and BJH models). It was proved that the adsorbent is amorphous, with a micrometric-sized, irregular-shaped particles and relatively large surface area of 540 m$^2$/g. Batch adsorption experiments were conducted to investigate the adsorption of Cd(II) ions on the prepared adsorbent, including evaluation of adsorption kinetics, the intraparticle diffusion model, the effect of pH, contact time, mass of the adsorbent, temperature and the effect of competitive Cl$^-$ and NO$_3^-$ anions. During the study, it was confirmed that the adsorption of Cd(II) ions reached equilibrium within 30 min, which was found to fit well with a pseudo-second-order kinetic model type 1 ($r^2 = 0.998$–$0.999$). The Mg–Si adsorbent exhibited high adsorption capacity for Cd(II) ions at pH above 7, and the maximum quantity of cadmium(II) ions adsorbed in optimal time was achieved for the highest metal ion concentrations: 18.22 (Cl$^-$) and 15.46 (NO$_3^-$) mg/g. The competitive anions present in the model cadmium salt solutions hindered adsorption in the sequence Cl$^-$>NO$_3^-$.

## Introduction

The development of industry and continuing urbanization brings about the generation of waste, which in turn is a source of toxic inorganic and organic substances that migrate freely in the environment, causing its degradation.

Among many technologies, which enable the removal of impurities from aqueous solutions, adsorption (Du et al. 2011; Salam and Burk 2010; Zheng et al. 2009), ion exchange, photocatalysis, filtration, coagulation, chemical precipitation, and electrodialysis or reverse osmosis (Chen et al. 2012; Gupta et al. 2012a, b, c; Maturana et al. 2011; Mungray et al. 2012), can be mentioned. Nonetheless, it is the adsorption process that provides scientists with a full spectrum of possibilities, in view of the wide range of available adsorbents supplied by nature ("natural adsorbents") and waste materials both known as *low-cost adsorbents* (Gupta and Nayak 2012; Jain et al. 2003; Mittal et al. 2009a, b, 2010a, b). The continual development of technologies enabling the production of synthetic systems, including recycling of waste materials, with specific porous structure parameters (synthetic adsorbents) is also very important (Saleh et al. 2013, 2014). Synthetic adsorbents have particular physicochemical properties that are produced in the course of their synthesis (Kiani et al. 2011; Lakshmi et al. 2009; Zhang et al. 2010). There are many reports in the literature concerning how the method of

✉ F. Ciesielczyk
Filip.Ciesielczyk@put.poznan.pl

[1] Faculty of Chemical Technology, Institute of Chemical Technology and Engineering, Poznan University of Technology, Berdychowo 4, 60965 Poznan, Poland

🖄 Springer

production and type of compound used as an adsorbent affect the efficiency of removal of, for instance, organic or inorganic impurities from aqueous systems (Bamgbose et al. 2010; Govindarajan et al. 2011; Ozdemir et al. 2004; Rangel-Mendez and Streat 2002; Srinivasa et al. 2010). The properties of adsorbents can be modified in various ways, including the creation of novel composite materials. Those composites are obtained by combining at least two components having different properties (Deng et al. 2010; Gupta et al. 2011a, b, c; Ren et al. 2011; Zheng et al. 2009). Substances are usually combined with the aim of enhancing a material by introducing features possessed by another adsorbent (Saleh et al. 2011; Saleh and Gupta 2012a, b). This group of materials includes composites based on chitosan, chitin and lignin, as well as aluminium oxide, titanium oxide, oxide systems and carbon nanotubes (Ciesielczyk et al. 2013; Gao et al. 2004; Gupta et al. 2009, Salam and Burk 2010). A novel hybrid material dedicated for environmental application might be a combination of multi-walled carbon nanotubes with titanium dioxide or tungsten utilized for photodegradation of selected organic dyes (Saleh and Gupta 2011, 2012a, b) and with iron oxide, alumina or manganese oxide utilized for hazardous metal ions removal present in wastewaters (Gupta et al. 2011a, b, c; Saleh et al. 2011; Saleh and Gupta 2012a, b). Those materials can be an alternative for commonly utilized oxide adsorbents and photocatalyst such as pure titania (Gupta et al. 2011a, b, c, 2012a, b).

The many reports concerning scientific research into sorbents provide an indication of how important it is to design the adsorption process correctly, the through determination of the impact of external factors on that process. The efficiency of adsorption of specified impurities is affected not only by the type of sorption material used, but also by the conditions in which the process takes place, such as temperature, reagent contact time, concentration of the impurities, pH and liquid-to-solid ratio (Gupta et al. 2012a, b, c; Ru et al. 2011; Sadeghi and Sheikhzadeh 2009; Wu et al. 2007).

Another important tool contributing to improvement of the process is the analysis of adsorption kinetics. This enables determination of how the rate of adsorption depends on the properties of the adsorbent itself and on the conditions under which the adsorption process takes place (Debnath and Ghosh 2011; Gupta et al. 2012a, b, c; Ho and McKay 1999; Moreno-Pirajan et al. 2011; Okasha et al. 2012; Plazinski et al. 2009; Souag et al. 2009).

In view of the rapid development of industry and continuing need for new multifunctional materials, an attempt was made to produce Mg–Si hybrid oxide adsorbents with defined physicochemical properties, including, in particular, specified porous structure parameters. The

adsorbent, which exhibits high sorption capacity with respect to Cd(II) ions, was prepared via the modified co-precipitation method and was thoroughly analysed. Batch sorption behaviours, including sorption kinetics as well as the effect of pH, contact time, mass of the adsorbent, temperature and competitive anions, were investigated in details.

The adsorption of cadmium(II) ions from their model, water solutions using novel, Mg–Si binary oxide adsorbent, was investigated in a 10-month period between May 2013 and February 2014, on laboratory scale at Poznan University of Technology, Institute of Chemical Technology and Engineering, Poznan, Poland.

## Materials and methods

### Preparation and characterization of Mg–Si hybrid oxide adsorbent

The Mg–Si hybrid oxide adsorbent was obtained in a modified co-precipitation method utilizing aqueous solutions of sodium silicate and magnesium sulphate, as described in previous reports (Ciesielczyk et al. 2011, 2013). An appropriate quantity (4 L) of 5 % solution of magnesium sulphate was placed in a reactor (10 L in capacity, QVF MiniPlant) equipped with a mechanical stirrer (Eurostar, IKA Werke), to which the same quantity of 5 % solution of sodium silicate was dosed at a rate of 1 L/h, utilizing peristaltic pump. The whole system was continuously stirred, even when the sodium silicate solution was completely introduced to the reactor. The synthesis last 5 h, and it was realized at room temperature. After precipitation, the product was filtered under reduced pressure, washed three times with distilled water and classified utilizing the sieve (80 μm). The chemical composition of the synthetic material (content of Mg, Si and O) was analysed utilizing atomic absorption spectroscopy (AAS), with the use of a Z-8200 spectrometer (Hitachi). To perform this analysis, 1 g of the resulting material was leached in a HCl:H$_2$O (1:1 v/v) solution for 1 h. After that time the mixture was filtrated, the sediment was dried and subjected to gravimetric analysis to evaluate the SiO$_2$ content, while the filtrate underwent AAS analysis to determine the Mg content. Additionally, for precise determination of the composition of the obtained powder materials, the moisture content was determined (drying at 105 °C for 2 h). To support these results, the surface composition of the prepared powder material was analysed utilizing energy dispersive X-ray spectroscopy (EDS), with the use of a Princeton Gamma-Tech unit with a prism digital spectrometer. The prepared Mg–Si hybrid also underwent crystalline structure determination using the WAXS

method. Diffraction patterns were taken using a TUR-M62 horizontal diffractometer equipped with an HZG-3 type goniometer, and the results were analysed with the use of X-Rayan software. The dispersive characteristics, morphology and microstructure of the material obtained were analysed using both a Mastersizer 2000 (Malvern Instruments Ltd.) and a Zeiss EVO40 scanning electron microscope. The observations enabled evaluation of the degree of dispersion, the structure of particles and their tendency towards aggregation or agglomeration. The surface area $A_{BET}$ (BET model) as well as pore volume and diameter (BJH model) were calculated based on data measured by low-temperature adsorption of nitrogen. The isotherms of nitrogen adsorption/desorption were measured at −196 °C using an ASAP 2020 apparatus (Micromeritics Instrument Co.). FTIR spectral analysis was performed using a Vertex 70 (Bruker). The samples were analysed in the form of tablets, made by pressing a mixture of anhydrous KBr (ca. 0.25 g) and 1 mg of the tested substance in a special steel ring, under a pressure of approximately 10 MPa. Analysis was performed over a wavenumber range of 4000–400 cm$^{-1}$ (at a resolution of 0.5 cm$^{-1}$, number of scans: 64).

As a result of this process, the binary oxide adsorbent was obtained characterized with micrometre-sized particles, an amorphous structure, mesoporous character and a relatively large BET surface area.

## Sorption experiments

Sorption experiments were conducted to investigate the adsorption of Cd(II) ions on the binary Mg–Si oxide adsorbent. All sorption experiments were carried out in 250-mL flasks, to which an appropriate amount of adsorbent and 100 mL of Cd(II) ions solution were added. Two different cadmium salts, with different competitive anions ($CdCl_2 \cdot 2.5H_2O$ and $Cd(NO_3)_2 \cdot 4H_2O$) were used as cadmium(II) ions precursors. This made it possible to evaluate the sequence of hindrance by competitive anions. The mixture was next stirred at 200 rpm using a magnetic stirrer (RO10, IKA Werke) for 1–240 min. Sorption behaviour, including contact time, effect of pH, mass of the adsorbent, temperature, sorption kinetics and competitive anions, was investigated in details. To evaluate the pH effect, measurements were performed with the initial pH of the solution ranging from 2 to 11, and with the initial Cd(II) ions concentration in the range of 25–100 mg/L. To obtain the desired pH, as monitored using a pH meter (CP-401, Elmetron), sodium hydroxide or an appropriate acid (HCl or $HNO_3$), in 0.1 M solution, was added. In order to establish the optimal mass of the adsorbent (1–10 g/L), the study was realized within 60 min utilizing model solutions of cadmium ions in the initial concentration of 50 mg/L.

The effect of the temperature on the efficiency of cadmium(II) ions adsorption was studied by carrying out the batch adsorption tests in temperature range of 20–30 °C within 60 min (at constant cadmium ions concentration of 50 mg/L). In the investigation of adsorption kinetics, Cd(II) ions solutions with initial concentration of 25–100 mg/L and pH = 7.5 were used, in an amount of 100 mL. After adsorption, the adsorbent was separated by filtration, and the final concentration of Cd(II) ions in the solution was determined. In order to determine the stability of bonds between the adsorbate and the adsorbent, and to determine the effectiveness of the removal of Cd(II) ions from the surface of the adsorbent, elution tests with $H_2O$ were performed. AAS analysis was performed to evaluate the quantity of Cd(II) ions present in the filtrate after the adsorption process and elution tests. This is one of the most accurate methods for quantitative analysis. This study was carried out using a Z-8200 spectrometer (Hitachi). Before analysing, a calibration curve was prepared to enable calculation of the Cd(II) ions concentration in the filtrate. The measurements were performed to an accuracy of ±0.1 mg/L. Additionally, the adsorbents after the process underwent EDS analysis, to evaluate the presence of Cd(II) in their structure.

Determination of adsorption kinetics of cadmium(II) ions was an important part of the experiments. Calculations were performed to determine the value $q_t$, which is needed in order to define various kinetic models: pseudo-first order (Lagergren 1898), pseudo-second order (Ho and McKay 1999) and the intraparticle diffusion model of Weber and Morris (1963). The quantity of metal ions adsorbed per unit time ($q_t$) on the adsorbent surface was computed using Eq. (1):

$$q_t = \frac{(C_0 - C_t) \cdot V}{m} \tag{1}$$

where $C_0$ and $C_t$ are the concentrations of cadmium(II) ions in the solution before and after sorption, respectively (mg/L), $V$ is the volume of the solution (L), and $m$ is the mass of adsorbent (g).
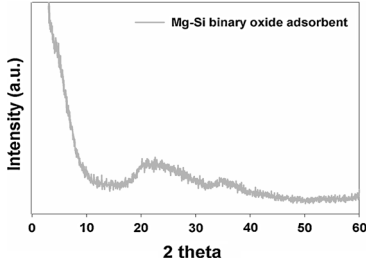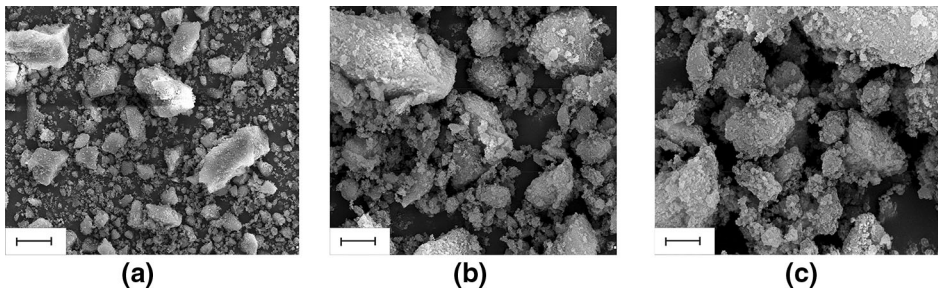
## Results and discussion

### Adsorbent characterization

In the first stage of the study, the physicochemical characteristic of the adsorbent—a precipitated Mg–Si hybrid—was investigated (Table 1). Analysis of the chemical composition of the Mg–Si hybrid proved the presence of two dominant components in its structure: $SiO_2$ (54.1 %) and MgO (20.4 %) as well as a certain amount of moisture (22.8 %). However, this amount can be reduced by the

**Table 1** Physicochemical characteristic of Mg–Si binary oxide adsorbent

| Adsorbent characteristic | |
| --- | --- |
| Chemical composition | |
| *Mg(II) (mg/L)—AAS analysis | 2120 |
| MgO (%) calculated from* | 20.4 |
| $SiO_2$ (mass%)—gravimetric analysis | 54.1 |
| $H_2O$—moisture (mass%)—gravimetric analysis | 22.8 |
| Surface composition | |
| MgO (mass%)—EDS analysis | 25.8 |
| $SiO_2$ (mass%)—EDS analysis | 56.4 |
| Crystalline structure | |



| Dispersive parameters (μm) | |
| --- | --- |
| $d(0.1)$ | 3.7 |
| $d(0.5)$ | 7.0 |
| $d(0.9)$ | 13.1 |
| D[4.3] | 7.8 |
| SEM image in the scale of (a) 10 μm, (b) 3 μm and (c) 2 μm | |



| Parameters of porous structure | |
| --- | --- |
| $A_{BET}$ ($m^2$/g) | 540 |
| $V_p$ (mL/g) | 0.49 |
| $S_p$ (nm) | 4.5 |

* Results obtained from AAS analysis

selection of an appropriate heat treatment technique, which directly determines the surface activity, translating into a number of reactive silanol and magnesil groups ($\equiv$Si–OH and –Mg–OH). It means that, taking into account average results from AAS and EDS analyses, adsorbent elements (MgO:$SiO_2$) ratio is 1:2.5. Due to the preparation of the synthetic Mg–Si hybrid in the laboratory, it was necessary to determine its crystalline structure. The results showed that the resulting oxide system has a completely amorphous structure. The nature of the adsorbent dispersion presented in the SEM photograph confirms the presence of micrometric-sized and irregular-shaped particles with mean diameter approximately of 7.8 μm. Using the synthetic Mg–Si oxide hybrid as a selective adsorbent, it was also necessary to determine the parameters of the porous structure. The synthetic Mg–Si hybrid is characterized with a significant surface area of 540 $m^2$/g, pore volume $V_p$ = 0.49 mL/g and pore diameter $S_p$ = 4.5 nm. The values of these parameters indicate the mesoporous character of the adsorbent.

## Sorption process

The efficiency of adsorption of cadmium(II) ions on the inorganic oxide system was determined chiefly on the basis of AAS analysis. Another important method for measuring the effectiveness of adsorption is EDS technique, which confirmed the successful removal of cadmium(II) ions from aqueous solutions by detection of cadmium in the adsorbent structure.

At first, the results of tests carried out to determine the optimum time of cadmium ion adsorption, for various precursors of that metal, are presented (Fig. 1).

Analysis of the dependences obtained (Fig. 1) proved that the adsorption of Cd(II) ions initially runs at a very fast rate, in the case of utilizing chloride as well as nitrate systems. In both cases, the equilibrium of adsorption was reached after 30 min. The maximum quantity of cadmium(II) ions adsorbed from its model solutions (with concentration of 25–100 mg/L) was obtained by continuing the process for 60 min and utilizing the highest metal ion concentration: 18.22 ($Cl^-$) and 15.46 ($NO_3^-$) mg/g. After that time, no significant changes in the quantity of adsorbed metal ions were noted. It means that cadmium(II) ions were therefore more effectively removed from chloride solutions, irrespective of the model solution concentrations tested (25–100 mg/L).

The results (Table 2; Fig. 2) showed the higher pH and the lower concentration of Cd(II) ions that there is an increase in the efficiency of their removal. Once again, Cd(II) ions were adsorbed much more favourably from chloride solutions. It may be explained by the greater solubility of cadmium chloride in aqueous solutions, which may have significantly facilitated their adsorption on the inorganic Mg–Si oxide system.

Experimental data demonstrate that increasing the pH of the reaction system to 7.5 enabled an increase of as much as 22 % in the efficiency of the process. It should be noted that

reaction systems with pH = 7.5 are a natural environment in which aqueous solutions of cadmium chloride and nitrate occur. A further increase in pH leads to an increase in the process efficiency by a further 10 %. When cadmium(II) ions were adsorbed from nitrate solution in the concentration of 25 mg/L at pH = 11, a process efficiency of 96.7 % was obtained. In turn, in the case of cadmium chloride, the highest efficiency of Cd(II) ions removal, equal to 98.9 %, was already reached at pH = 9. In this case, further increase in the pH of the reaction system did not lead to any increase in the adsorption efficiency.

The tests showed that the pH of the reaction system has a significant effect on the efficiency of adsorption of cadmium(II) ions on an inorganic Mg–Si binary oxide adsorbent. Cadmium(II) ions were most weakly adsorbed in an acidic environment. Low pH values are unfavourable for their adsorption, since in that range they are present in solution in free form as $Cd^{2+}$ (irrespective of the type of precursor used); hence, in this case there is electrostatic repulsion between the cation and the positively charged surface of the adsorbent. With an increase in pH, and with a decrease in protonation of the Mg–Si hybrid oxide adsorbent, the cadmium(II) ions bond with $OH^-$ groups, finally forming cadmium hydroxide $Cd(OH)_2$, which settles very well in the pores of the adsorbing material. In a strongly basic environment, however, the anions $Cd(OH)_3^-$ and $Cd(OH)_4^{2-}$ are formed. These forms of Cd(II), like cadmium hydroxide, strongly interact with the surface of the inorganic oxide adsorbent, making adsorption easier, which is in agreement with literature reports (Debnath and Ghosh 2009; Gao et al. 2004; Sheela and Nayaka 2012).

At the next stage, the adsorbent/adsorbate systems underwent EDS analysis (Table 2). The analysed systems were obtained following adsorption processes carried out at pH 2, 7.5 and 11, for Cd(II) ions concentration of 25, 50 and 100 mg/L.
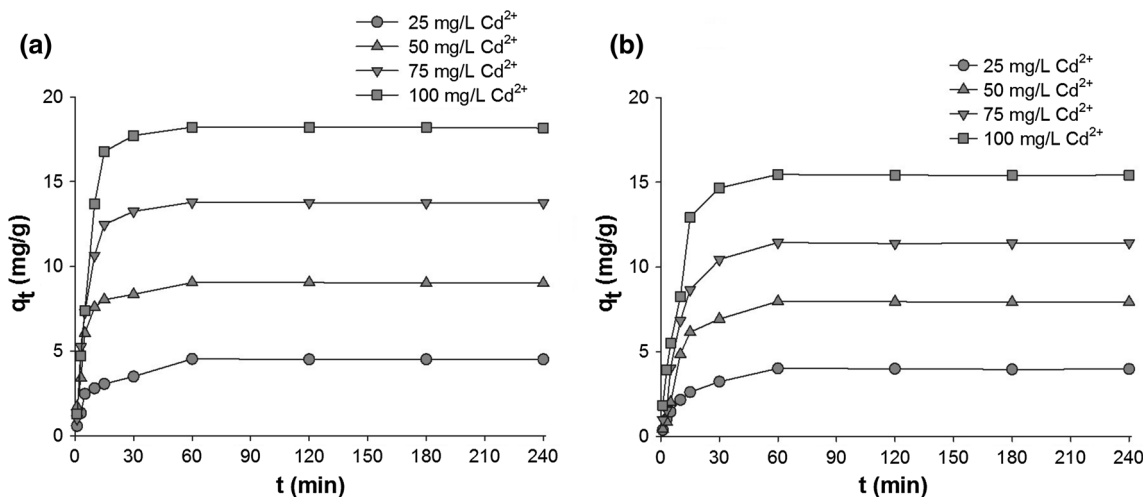


**Fig. 1** Quantity of cadmium(II) ions adsorbed versus time, using **a** chloride and **b** nitrate model solutions

3618

Int. J. Environ. Sci. Technol. (2015) 12:3613–3626

**Table 2** Influence of pH on the efficiency of adsorption of cadmium(II) ions (EDS analysis)

| pH | Concentration of Cd(II) ions (mg/L) | Element | mass% contribution | |
|----|-----|-----|-----|-----|
| | | | Precursor of Cd(II) ions | |
| | | | Cadmium chloride | Cadmium nitrate |
| 2 | 25 | Mg | 8.67 | 8.81 |
| | | Si | 39.87 | 39.93 |
| | | **Cd** | **0.08** | **0.06** |
| | | O | 51.40 | 51.18 |
| | 50 | Mg | 8.89 | 8.73 |
| | | Si | 39.20 | 39.30 |
| | | **Cd** | **0.08** | **0.07** |
| | | O | 51.84 | 51.89 |
| | 100 | Mg | 9.23 | 8.85 |
| | | Si | 39.21 | 39.94 |
| | | **Cd** | **0.09** | **0.07** |
| | | O | 51.49 | 51.12 |
| 7.5 | 25 | Mg | 8.89 | 8.89 |
| | | Si | 39.27 | 39.20 |
| | | **Cd** | **0.20** | **0.16** |
| | | O | 51.68 | 51.71 |
| | 50 | Mg | 8.86 | 9.03 |
| | | Si | 39.80 | 39.10 |
| | | **Cd** | **0.36** | **0.23** |
| | | O | 51.11 | 51.51 |
| | 100 | Mg | 8.85 | 8.78 |
| | | Si | 39.45 | 39.98 |
| | | **Cd** | **0.80** | **0.71** |
| | | O | 51.68 | 51.71 |
| 11 | 25 | Mg | 8.24 | 8.27 |
| | | Si | 40.88 | 40.46 |
| | | **Cd** | **0.24** | **0.23** |
| | | O | 50.65 | 51.03 |
| | 50 | Mg | 8.71 | 8.80 |
| | | Si | 39.81 | 39.27 |
| | | **Cd** | **0.88** | **0.43** |
| | | O | 51.04 | 51.05 |
| | 100 | Mg | 8.83 | 8.87 |
| | | Si | 38.68 | 38.67 |
| | | **Cd** | **0.96** | **0.91** |
| | | O | 51.58 | 51.50 |

Bold values indicate the amount of cadmium present in the oxide adsorbent structure

Collected data indicate a negligible adsorption of cadmium(II) ions in an acidic environment, confirming the results obtained by AAS analysis. A low pH of the reaction system effectively suppresses the adsorption of cadmium(II) ions. The highest content of Cd(II) in the adsorbent structure, equal to 0.09 % by mass, was obtained when adsorption took place from a model solution of $CdCl_2$·$2.5H_2O$ with Cd(II) ions concentration of 100 mg/L. When cadmium nitrate, with the same concentration of cadmium(II) ions, was used, a maximum content of 0.07 % by mass was obtained—Cd(II) was deposited on the surface and in the pores of the tested binary oxide adsorbent.

The amount of cadmium in the structure of Mg–Si oxide adsorbent increased together with an increase in the concentration of Cd(II) ions in model solutions. Moreover, increasing the pH of the reaction system to 7.5 also caused an increase in cadmium content in tested adsorbent samples up to 0.80 and 0.71 % by mass, utilizing model chloride and nitrate solutions containing 100 mg/L of Cd(II) ions, respectively. A further increase in the pH of the reaction system (pH = 11) enabled a significant improvement in the removal of cadmium(II) ions from its model solutions. EDS analysis showed that Cd(II) ions were more favourably adsorbed from chloride than from nitrate solutions (0.96 and 0.91 % by mass of cadmium evaluated in Mg–Si adsorbent structure after its adsorption from model solution containing 100 mg/L of Cd(II) ions). By comparing these results with those obtained in an acidic environment, where the mass content of Cd(II) in the structure of the Mg–Si binary oxide adsorbent was 0.04–0.09 %, it can be concluded that pH of the reaction system has an enormous effect on the efficiency of adsorption of this metal ions.

Figure 3a presents the influence of adsorbent mass on the efficiency of adsorption. It was rather obvious that by increasing mass of binary Mg–Si oxide adsorbent, the effectiveness of removal of Cd(II) ions will be higher. The same situation was observed for both cadmium ions precursors. The highest efficiencies of adsorption (97 and 88 %, for chloride and nitrate cadmium ions precursors, respectively) were noted for the highest mass (10 g/L) of the adsorbent.

Additionally, the effect of temperature on cadmium ions removal from their model solutions was estimated (Fig. 3b). Dependences obtained clearly confirmed that this parameter does not affect the efficiency of realized process of adsorption. There were no significant changes in efficiency of adsorption in the studied temperature range (20–30 °C), and that is why all experiments were realized at room temperature.

Figure 4 presents the FTIR spectra of analysed adsorbent samples. The FTIR spectra of all samples show the signals characteristic for Mg–Si binary oxide adsorbent, which are in agreement with the literature (Moscofian et al. 2012). A clear, broad signal at a wavenumber of 3650–3350 $cm^{-1}$ is generated by the stretching vibration of hydroxyl groups. In turn, the band with significant intensity, with a maximum at about 1050 $cm^{-1}$, is characteristic for the stretching vibration of Si–O. Visible are also clear signals at 480 $cm^{-1}$, originating from the deformation vibration of Mg–O bonds. Additionally, the signal that appears at around 800 $cm^{-1}$ is
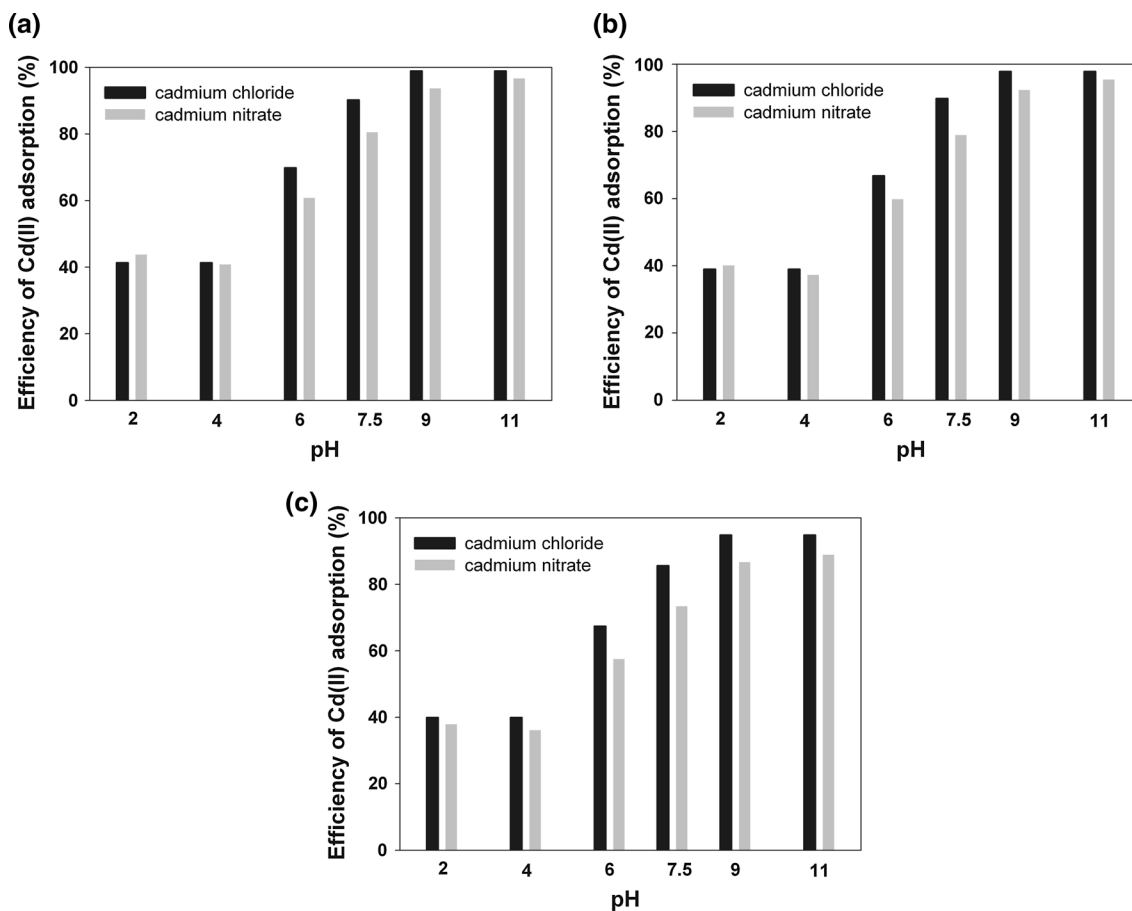
**Fig. 2** Efficiency of cadmium(II) ions adsorption versus pH using chloride and nitrate model solutions with Cd(II) ions concentration of **a** 25 mg/L, **b** 50 mg/L and **c** 100 mg/L ($t = 60$ min)

related to the stretching vibration of O–Mg–O bonds, and this one at 667 cm$^{-1}$ is characteristic for the stretching vibration of Si–O–Mg bonds. The presence of other bands specific for the analysed adsorbent is somewhat masked by the presence of significant quantities of water in its structure, which can be confirmed by a signal appearing at 1630 cm$^{-1}$ related to bending vibrations derived from water molecules that have been physically adsorbed on the surface of the resulting powder. Slight decrease in the intensity of bands especially in the range of 3650–3350 cm$^{-1}$ for adsorbent samples after adsorption of cadmium(II) ions from their model chloride and nitrate solutions in the concentration of 50 mg/L at pH = 7.5 was observed. This dependence can be an evidence for the substitution of Mg–Si surface hydroxyls with Cd(II).

## Sorption kinetics

When adsorption technique is to be applied, it is necessary to investigate its kinetics, to enable precise design of the process. Models of kinetics, based on the quantity of adsorbed substance as a function of time, have been proposed

in previous reports (Alyüz and Veli 2009; Li et al. 2007). To determine the rate constant of the adsorption process, the equations of Lagergren's pseudo-first-order kinetic model, Ho's pseudo-second-order kinetic model and the intraparticle diffusion model of Weber and Morris were used. Due to the fact that the better results of adsorption efficiency were obtained utilizing cadmium chloride model solutions, these data were used to define adsorption kinetics.

## Pseudo-first-order kinetic model

A linear model of the pseudo-first-order adsorption kinetics is defined by Lagergren's Eq. (2):

$$\log(q_e - q_t) = \log q_e - \frac{k_1}{2.303} \cdot t \qquad (2)$$

where $q_e$ and $q_t$ (mg/g) are the quantities of cadmium(II) ions adsorbed at equilibrium and at time $t$ (min), respectively, and $k_1$ (1/min) is the rate constant for the pseudo-first-order model. The equilibrium adsorption capacity ($q_e$) and adsorption rate constant ($k_1$) (Table 3) can be

3620

Int. J. Environ. Sci. Technol. (2015) 12:3613–3626
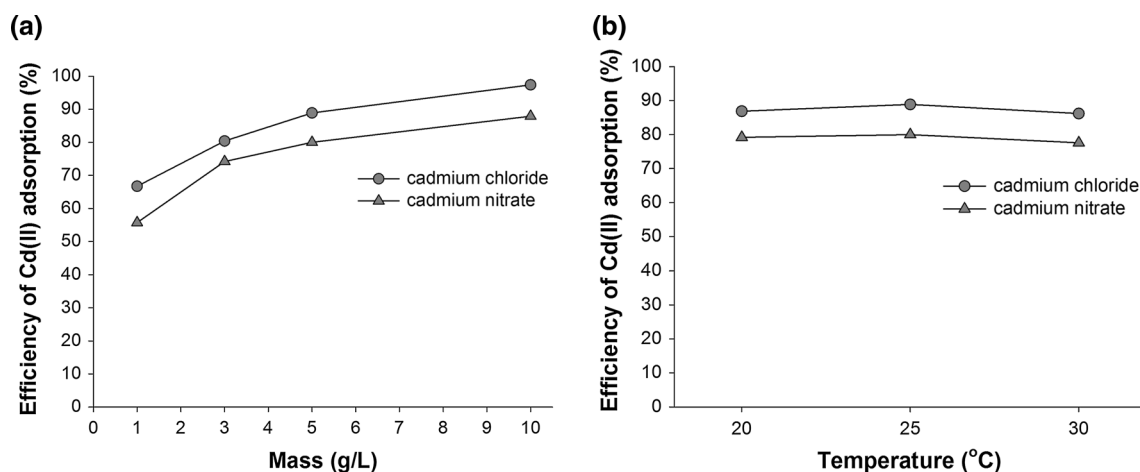
**(a)**



**(b)**

**Fig. 3** Effect of **a** adsorbent mass and **b** temperature on the efficiency of Cd(II) ions removal from both chloride and nitrate model solution
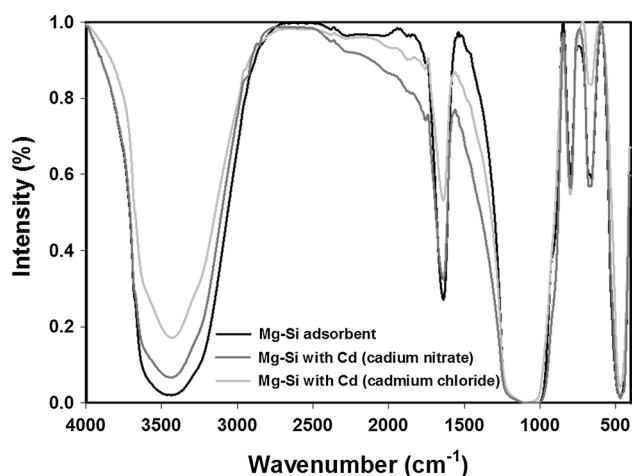


**Fig. 4** FTIR spectra of the analysed Mg–Si binary oxide adsorbents before and after adsorption of cadmium(II) ions from their model chloride and nitrate solutions in the concentration of 50 mg/L at pH = 7.5

computed experimentally by plotting $\log(q_e - q_t)$ against $t$. A graph of $\log(q_e - q_t)$ versus $t$ for the pseudo-first-order case is shown in Fig. 5. Table 3 gives the values of the adsorption rate constant ($k_1$) for particular concentrations of cadmium(II) ions, calculated from the gradients in Fig. 5. It was noted that the rate constants of the adsorption processes for the cadmium(II) ions concentration studied (25–100 mg/L) lay in the range of 0.021–0.034. The correlation coefficient is found to increase with a rise in the concentration of cadmium(II) ions, starting at 0.805 and reaching 0.985. However, the results for adsorption capacity ($q_{e,cal}$) obtained based on the pseudo-first-order kinetic model calculations deviated significantly from the values of the experimental capacities ($q_{e,exp}$). Much better results were obtained using the pseudo-second-order kinetic model.

### Pseudo-second-order kinetic model

A linear model of the pseudo-second-order adsorption kinetics is defined by Eq. (3):

$$\frac{t}{q_t} = \frac{1}{k_2 \cdot q_e^2} + \frac{1}{q_e} \cdot t \tag{3}$$

where $k_2$ (g/mg min) is the rate constant for the pseudo-second-order rate equation, and $q_e$ and $q_t$ are the quantities (mg/g) of cadmium(II) ions adsorbed at equilibrium and at time $t$ (min).

The initial adsorption rate $h$ (g/mg min) is defined as follows:

$$h = k_2 \cdot q_e^2 \tag{4}$$

The values $k_2$ and $q_e$ may be determined from the gradient and intercept, respectively, of the plot of $t/q_t$ versus $t$. This relationship can be classed as a type 1 pseudo-second-order kinetic model. There are other subtypes of pseudo-second-order model, which can also be used to compute the values $k_2$ and $q_e$.

Plotting the above curves (Fig. 6) makes it possible to estimate the model value of the concentration of adsorbate on the adsorbent surface and the rate constants ($k_2$) for saturation of the sorption capacity of the Mg–Si binary oxide system (Table 3).

The kinetics of the adsorption of cadmium(II) ions from model solutions in concentration of 25, 50, 75 and 100 mg/L on an inorganic oxide adsorbent is very well described by the first type of pseudo-second-order kinetic model. This is confirmed by the high value of the correlation coefficient ($r^2$), which was 0.999 (Table 3) for initial cadmium(II) ions concentration of 25 and 50 mg/L, and 0.998 for the model solutions with concentration of 75 and 100 mg/L. The decrease in the rate constant of the adsorption process ($k_2$) was also observed, as the initial concentration of

cadmium(II) ions increased. The adsorption capacity ($q_{e,cal}$) obtained from the type 1 of pseudo-second-order kinetic equation corresponded well with the experimental capacities ($q_{e,exp}$). The parameters obtained indicate clearly the good possibility of using a type 1 of pseudo-second-order model for predicting the kinetics of cadmium ion adsorption on Mg–Si binary oxide adsorbent.

For the remaining types (2–3) of pseudo-second-order kinetic models, the correlation coefficient lies in the range of 0.953–0.993. However, the adsorption capacities ($q_{e,cal}$) computed based on the type 2 and 3 of pseudo-second-order kinetic models did not correspond to the experimental capacities ($q_{e,exp}$). The values of $q_{e,cal}$ were significantly higher, particularly for cadmium(II) ions concentrations of 75 and 100 mg/L. The values obtained for the rate constant of the adsorption process ($k_2$) were also low (0.0003–0.001) for these model solutions of cadmium(II) ions. The parameters determined using the type 2 and 3 of pseudo-second-order models indicate the impossibility of using those models to obtain a correct description of the adsorption kinetics of cadmium(II) ions on a synthesized Mg–Si adsorbent.

In the case of the type 4 of pseudo-second-order kinetic model (Fig. 6d; Table 3), unfavourable results were obtained. This is confirmed by the value of the correlation

coefficient ($r^2$), which for all initial concentrations of cadmium(II) ions (25, 50, 75 and 100 mg/L) lay in the range of 0.355–0.904. It should be also noted that for model concentrations of 50 and 100 mg/L, negative values of $k^2$ (the adsorption rate constant) and the coefficient $h$ were obtained, which were not achievable experimentally.

Analysis of the porous structure of the sorbents used (Table 4) showed a reduction in their surface area and pore volume values, which may suggest that the adsorption process involves intraparticle diffusion. Consequently, the
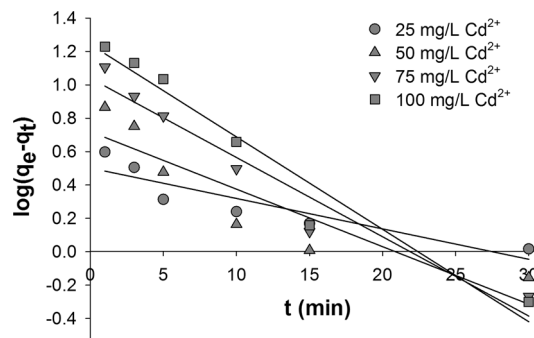
**Fig. 5** Pseudo-first-order kinetic fit for adsorption of cadmium(II) ions onto Mg–Si binary oxide adsorbent

**Table 3** Pseudo-first-order and pseudo-second-order kinetic parameters obtained using linear methods at different cadmium(II) ions concentration

| Type of kinetic | Parameter | | Concentration of Cd(II) ions (mg/L) | | | |
|---|---|---|---|---|---|---|
| | Symbol | Unit | 25 | 50 | 75 | 100 |
| Pseudo-first order | $q_{e,exp}$ | mg/g | 4.540 | 9.060 | 13.780 | 18.220 |
| | $q_{e,cal}$ | mg/g | 9.075 | 17.699 | 28.112 | 45.600 |
| | $k_1$ | 1/min | 0.021 | 0.030 | 0.034 | 0.029 |
| | $r^2$ | – | 0.805 | 0.860 | 0.941 | 0.985 |
| Pseudo-second order | | | | | | |
| Type 1 | $q_{e,cal}$ | mg/g | 4.676 | 9.168 | 14.109 | 18.790 |
| | $k_2$ | g/mg min | 0.033 | 0.039 | 0.016 | 0.009 |
| | $h$ | mg/g min | 0.729 | 3.271 | 3.079 | 3.261 |
| | $r^2$ | – | 0.999 | 0.999 | 0.998 | 0.998 |
| Type 2 | $q_{e,cal}$ | mg/g | 4.971 | 9.974 | 39.472 | 39.977 |
| | $k_2$ | g/mg min | 0.028 | 0.021 | 0.001 | 0.001 |
| | $h$ | mg/g min | 0.661 | 2.070 | 1.095 | 1.373 |
| | $r^2$ | – | 0.993 | 0.988 | 0.953 | 0.982 |
| Type 3 | $q_{e,cal}$ | mg/g | 5.017 | 10.083 | 57.834 | 44.131 |
| | $k_2$ | g/mg min | 0.0272 | 0.020 | 0.0003 | 0.001 |
| | $h$ | mg/g min | 0.656 | 2.043 | 1.043 | 1.349 |
| | $r^2$ | – | 0.991 | 0.987 | 0.953 | 0.982 |
| Type 4 | $q_{e,cal}$ | mg/g | 4.794 | 3.859 | 17.923 | 4.853 |
| | $k_2$ | g/mg min | 0.030 | −10.679 | 0.002 | −4.304 |
| | $h$ | mg/g min | 0.680 | −137.53 | 0.663 | −101.371 |
| | $r^2$ | – | 0.904 | 0.355 | 0.509 | 0.373 |

intraparticle diffusion model of Weber and Morris was used to investigate the diffusion mechanism:

$$q_t = k_t \cdot t^{0.5} + C \qquad (5)$$

where $k_t$ is the intraparticle diffusion rate (mg/g min$^{0.5}$), and $C$ is a constant enabling determination of the thickness of the boundary layer. According to this model, if the plot of $q_t$ versus $t^{0.5}$ (Fig. 7) is a straight line, then the adsorption of cadmium(II) ions onto the Mg–Si binary oxide adsorbent is controlled by intraparticle diffusion. In this case, for each concentration of model cadmium(II) ions solutions, there are two lines (multilinearity). In Fig. 7, it can be seen that the plots of $q_t$ versus $t^{0.5}$ obtained for cadmium(II) ions adsorption onto the Mg–Si adsorbent do not pass through the origin. This indicates that intraparticle diffusion is not the only rate-limiting mechanism. However, the dual linear character can be explained as follows: the first linearity relates to the total transport of cadmium(II) ions to the outer surface (layer) of the adsorbent, while the second linearity indicates diffusion of cadmium(II) ions to the internal surface of the pores of the synthetic Mg–Si binary oxide adsorbent.

## Elution tests

The degree of elution of cadmium from the surface of the Mg–Si binary oxide adsorbent using water (Table 5) shows its value to be practically zero. This holds for all concentrations of model solutions (25–100 mg/L) used in the first stage of the adsorption process, for both cadmium(II) ions precursors. This provides an evidence of the high stability of the interactions between cadmium(II) ions and the adsorbent surface and is in agreement with the relationships noted above.

Synthetic adsorbents offer very good physicochemical properties, which can be obtained thanks to laboratory work on specific systems. There are many reports concerning applications of synthetic systems in the removal of hazardous metal ions from aqueous solutions, including consideration of the parameters required to achieve favourable results for adsorption efficiency.

Gao et al. (2004) report a study of the use of anatase (a polymorphous variety of titanium(IV) dioxide) as an adsorbent of cadmium(II) ions from aqueous solutions. The main goal was to determine how the size of particles of the
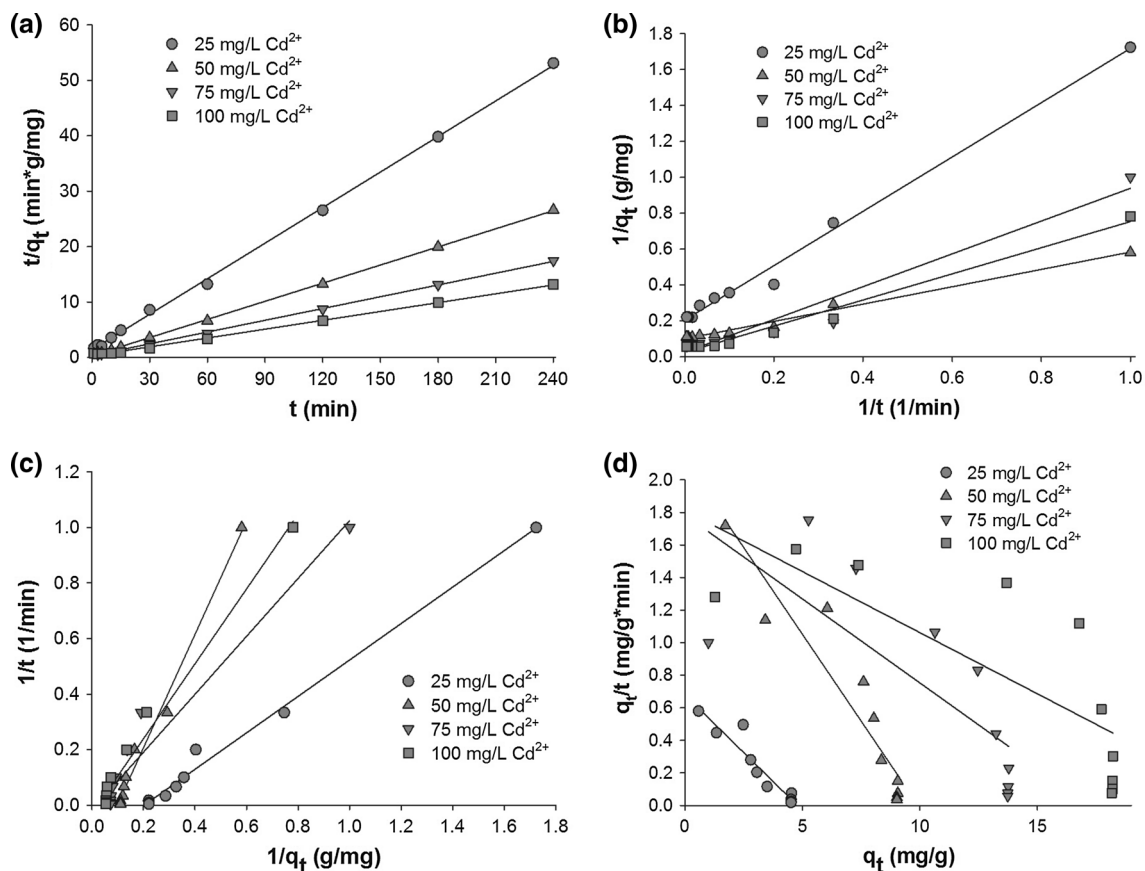


Fig. 6 Pseudo-second-order kinetic fit for adsorption of cadmium(II) ions onto Mg–Si binary oxide adsorbent: a type 1, b type 2, c type 3 and d type 4

**Table 4** Parameters of the porous structure of Mg–Si binary oxide adsorbents after realized process of adsorption

| Adsorbent | Adsorption conditions | | Parameters of the porous structure | | |
|---|---|---|---|---|---|
| | pH | Cd(II) ions concentration (mg/L) | $A_{BET}$ $(m^2/g)$ | $V_p$ (mL/g) | $S_p$ (nm) |
| Mg–Si binary oxide | – | – | 540 | 0.49 | 4.5 |
| | 2 | 100 | 502 | 0.36 | 3.1 |
| | 4 | | 488 | 0.28 | 2.8 |
| | 6 | | 484 | 0.27 | 2.8 |
| | 7.5 | | 484 | 0.28 | 2.8 |
| | 9 | | 467 | 0.27 | 2.8 |
| | 11 | | 442 | 0.27 | 2.8 |

**Table 5** Recovery of cadmium(II) ions from Mg–Si binary oxide adsorbent surface (elution tests with water)

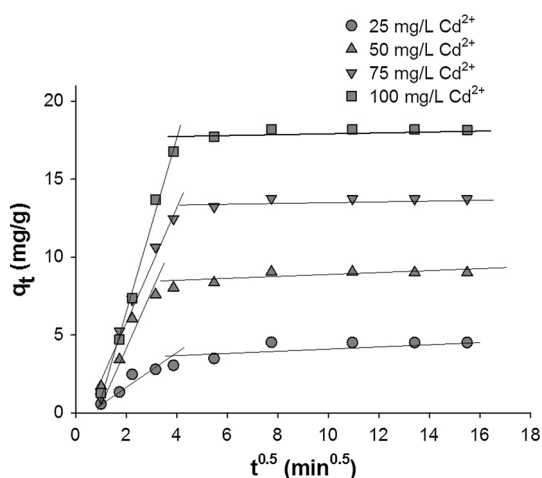| Initial metal ion concentration (mg/L) | Amount of cadmium ions adsorbed (mg/g) | | Recovery of metal ions (%) | |
|---|---|---|---|---|
| | Model chloride solution | Model nitrate solution | Model chloride solution | Model nitrate solution |
| 25 | 4.54 | 4.02 | 0.2 | 0.4 |
| 50 | 9.06 | 7.98 | 0.4 | 0.5 |
| 75 | 13.78 | 11.44 | 0.6 | 0.9 |
| 100 | 18.22 | 15.46 | 1.1 | 1.4 |



**Fig. 7** Effect of initial cadmium(II) ions concentration on the intraparticle diffusion kinetics of cadmium(II) ions on synthetic Mg–Si binary oxide adsorbent

material affects the efficiency of adsorption of Cd(II) ions. In order to describe this relationship accurately, solvothermal synthesis was used, where the conditions (raised pressure and temperature, different solvents and pH) enable precise crystallization of a material with an appropriate structure, and control of the particle morphology in terms of size and shape. Four different commercial samples of anatase were tested. Cadmium(II) ions were adsorbed from an aqueous solution of cadmium nitrate—Cd(NO₃)₂·4H₂O. Measurements showed that larger particles of anatase are much more effective in the removal of Cd(II) ions. This result was explained in terms of intraparticle electrostatic effects; nonetheless, the result is connected with the fact that this sample has the largest surface area out of all the anatase samples. The material was also tested to determine the effect of pH of the aqueous solution of adsorbate on the efficiency of the adsorption process. It was found that the adsorption efficiency

increases with increasing pH. Above pH = 7.0, an equilibrium is reached, and this is, therefore, an optimum value for the analysed system (Gao et al. 2004).

Another publication (Sheela and Nayaka 2012) describes the use of NiO nanoparticles as an adsorbent of cadmium and lead ions from aqueous solutions. The effect of such factors as time, pH and adsorbate concentration was investigated. The nanomaterial was obtained by precipitation and calcination (2 h, 600 °C). These operations produced a highly active material with a grain size of 28 nm. At the next stage, the nickel oxide was used in the process of adsorption of Cd(II) and Pb(II) ions from aqueous solutions of their salts CdCl₂·2H₂O and Pb(NO₃)₂. It was observed that with an increase in adsorption time, the quantity of the hazardous metals contained in the system successively decreased. It was found that after 60 min, equilibrium was reached, and this is, therefore, the optimum time for the adsorption of cadmium and lead by NiO nanoparticles. It was also shown that with an increase in the concentration of the metal ions in the system, the efficiency of the process increases. The results of adsorption efficiency for Cd(II) ions indicated that an increase in pH was extremely favourable for removal of the metal from solution. The highest process efficiency (90 %) was recorded for pH = 12. Lead ions required a much lower pH for the efficiency of their removal to reach 84 %. Further raising of pH in the case of Pb(II) ions led to a decrease in the efficiency of adsorption (Sheela and Nayaka 2012).

Adebowale et al. (2006) described the use of modified kaolinite as an adsorbent of cadmium and lead ions from aqueous solution. A determination was made of the effect of such factors as time, pH and adsorbate concentration on the adsorption efficiency. Ions of the hazardous metals were removed from aqueous solutions of cadmium nitrate and lead nitrate. The results confirmed that the efficiency of the process increases with increasing pH. Cadmium(II) ions were adsorbed most effectively at pH = 7.5. For lead ions, the most favourable results were recorded starting from pH = 5.5, after which an equilibrium was reached.

The concentration of hazardous metal ions was also of high significance. It was found that smaller quantities of cadmium and lead ions in aqueous solution allow the adsorption process to take place with greater effectiveness. It was also shown that equilibrium was reached after just 15 min for both hazardous metal ions (Adebowale et al. 2006).

The above review of the literature shows the importance of investigating the factors influencing the process of adsorption of selected inorganic impurities from aqueous solutions. Depending on the material itself, and also on the adsorbate, the system requires specific conditions in which it is possible to attain the most favourable results for adsorption efficiency. Much attention is also paid to adsorption materials. The development of modern technologies means that natural adsorbents can be modified, enabling the design of their most important properties such as surface area. Minor treatments can be used to improve synthetic materials. A simple change in the process for obtaining or modifying an adsorbent can often bring about an increase in its adsorption efficiency. Adsorption is an exceptional technique, which effectively reduces level of contamination in aqueous solutions. Nonetheless, in order to obtain the most favourable results, it is necessary to design the conditions of the adsorption process and also to make appropriate modifications to the adsorbent itself (Adebowale et al. 2006; Debnath and Ghosh 2009; Sheela and Nayaka 2012; Wang et al. 2012).

## Conclusion

The investigated properties of Mg–Si binary oxide adsorbent confirm its high level of activity and ability to adsorb hazardous metals ions (such as cadmium(II) ions) from aqueous solutions. The efficiency of adsorption was strongly dependent on the contact time of the reactants, on the type of metal ion precursor used and especially on the pH of the reaction medium.

It was found that an adsorption process lasting 30 min is sufficient to achieve equilibrium, irrespective of the type of cadmium(II) ions precursor and their concentration, but the maximum quantity of cadmium(II) ions adsorbed was obtained by continuing the process for 60 min. When comparing cadmium chloride solutions to the nitrate ones, the higher the concentration of model cadmium ions solution, the higher efficiency of their removal and the more effective adsorption. Moreover, adsorption of Cd(II) ions onto Mg–Si binary oxide adsorbent was less efficient at acidic than at neutral or alkaline pH. The highest degree of cadmium(II) ions removal from model chloride solutions (98.9 %) was already obtained at pH = 9 and from model nitrate solutions (96.7 %) at pH = 11. Further increase in

the pH of the reaction system did not lead to any increase in the adsorption of cadmium(II) ions. The presence of cadmium on the adsorbent surface (confirmed by EDS analysis) confirms the successfully performed experiment. Similarly, the lower intensity of bands related to the characteristic functional groups of Mg–Si oxide adsorbent (confirmed by FTIR spectra) indirectly confirms their substitution with Cd(II).

Additionally, increasing the mass of binary Mg–Si oxide adsorbent, it was possible to increase the effectiveness of Cd(II) ions removal, irrespective of the type of cadmium ions precursor.

Moreover, dependences obtained clearly confirmed that the temperature do not affect the efficiency of realized process of adsorption.

The mechanism of the adsorption process was well described by the equation of the first type of pseudo-second-order kinetic model ($r^2 = 0.999$ for Cd(II) ions concentration of 25 and 50 mg/L, and $r^2 = 0.998$ for concentration of 75 and 100 mg/L). Adsorption capacity ($q_{e,cal}$) calculated based on the type 1 of pseudo-second-order kinetic model corresponds with the values of experimental capacities ($q_{e,exp}$). The relationships obtained directly confirm the possibility of using the type 1 of pseudo-second-order model to predict the kinetics of adsorption of cadmium(II) ions onto Mg–Si binary oxide adsorbent.

The decrease in all porous structure parameters indicates that the adsorption process involves intraparticle diffusion, characterized firstly by total transport of cadmium(II) ions to the external adsorbent surface and then their diffusion to the internal surface of the pores. It should be noted that the bonds between cadmium(II) ions and the Mg–Si oxide adsorbent surface are very stable, as was confirmed by the elution tests. The amount of cadmium removed from the adsorbent surface increased together with increasing concentration of its precursors, utilized in adsorption process.

## References

Adebowale KO, Unuabonah IE, Olu-Owolabi BI (2006) The effect of some operating variables on the adsorption of lead and cadmium(II) ions on kaolinite clay. J Hazard Mater 134:130–139

Al-Saadi AA, Saleh A, Gupta VK (2013) Spectroscopic and computational evaluation of cadmium adsorption using activated carbon produced from rubber tires. J Mol Liq 188:136–142

Alyüz B, Veli S (2009) Kinetics and equilibrium studies for the removal of nickel and zinc from aqueous solutions by ion exchange resins. J Hazard Mater 167:482–488

Bamgbose JT, Adewuyi S, Bamgbose O, Adetoye AA (2010) Adsorption kinetics of cadmium and lead by chitosan. Afr J Biotechnol 9:2560–2565

Chen YX, Zhong BH, Fang WM (2012) Adsorption characterization of lead(II) and cadmium(II) on crosslinked carboxymethyl starch. J Appl Polym Sci 124:5010–5020

Ciesielczyk F, Nowacka M, Przybylska A, Jesionowski T (2011) Dispersive and electrokinetic evaluations of alkoxysilane-modified MgO–SiO$_2$ oxide composite and pigment hybrids supported on it. Colloids Surf A Physicochem Eng Asp 376:21–30

Ciesielczyk F, Bartczak P, Wieszczycka K, Siwińska-Stefańska K, Nowacka M, Jesionowski T (2013) Adsorption of Ni(II) from model solutions using co-precipitated inorganic oxides. Adsorption 19:423–434

Debnath S, Ghosh UC (2009) Nanostructured hydrous titanium(IV) oxide: synthesis, characterization and Ni(II) adsorption behavior. Chem Eng J 152:480–491

Debnath S, Ghosh UC (2011) Equilibrium modeling of single and binary adsorption of Cd(II) and Cu(II) onto agglomerated nanostructured titanium(IV) oxide. Desalination 273:330–342

Deng S, Li Z, Huanga J, Yua G (2010) Preparation, characterization and application of a Ce–Ti oxide adsorbent for enhanced removal of arsenate from water. J Hazard Mater 179:1014–1021

Du Y, Lian F, Zhu L (2011) Biosorption of divalent Pb, Cd and Zn on aragonite and calcite mollusk shells. Environ Pollut 159:1763–1768

Feng L, Cao M, Ma X, Zhu Y, Hu C (2012) Superparamagnetic high-surface area Fe$_3$O$_4$ nanoparticles as adsorbents for arsenic removal. J Hazard Mater 217:439–446

Gao Y, Wahi R, Kan AT, Falkner JC, Colvin VL, Tomson MB (2004) Adsorption of cadmium on anatase nanoparticles effect of crystal size and pH. Langmuir 20:9585–9593

Gao C, Zhang W, Li H, Lang L, Xu Z (2008) Controllable fabrication of mesoporous MgO with various morphologies and their absorption performance for toxic pollutants in water. Cryst Growth Des 8:3785–3790

Govindarajan C, Ramasubramaniam S, Gomathi T, Sudha PN (2011) Studies on adsorption behavior of cadmium onto nanochitosan carboxymethyl cellulose blend. Arch Appl Sci Res 3:572–580

Gupta VK, Gosh UC (2009) Arsenic removal using hydrous nanostructure iron(III)–titanium(VI) binary mixed oxide from aqueous solution. J Hazard Mater 161:884–892

Gupta VK, Nayak A (2012) Cadmium removal and recovery from aqueous solutions by novel adsorbents prepared from orange peel and Fe$_2$O$_3$ nanoparticles. Chem Eng J 180:81–90

Gupta VK, Jain R, Nayak A, Agarwal S, Shrivastava M (2011a) Removal of the hazardous dye—tartrazine by photodegradation on titanium dioxide surface. Mater Sci Eng C 31:1062–1067

Gupta VK, Agarwal S, Saleh TA (2011b) Chromium removal by combining the magnetic properties of iron oxide with adsorption properties of carbon nanotubes. Water Res 45:2207–2212

Gupta VK, Agarwal S, Saleh TA (2011c) Synthesis and characterization of alumina-coated carbon nanotubes and their application for lead removal. J Hazard Mater 185:17–23

Gupta VK, Jain R, Mittal A, Saleh TA, Nayak A, Agarwal S, Sikarwar S (2012a) Photo-catalytic degradation of toxic dye amaranth on TiO$_2$/UV in aqueous suspensions. Mater Sci Eng C 32:12–17

Gupta VK, Bhattacharya S, Chattopadhyay D, Mukhopadhyay A, Biswas H (2012b) Ceria associated manganese oxide nanoparticles: synthesis, characterization and arsenic(V) sorption behavior. Chem Eng J 172:219–229

Gupta VK, Ali I, Saleh TA, Nayak A, Agarwal S (2012c) Chemical treatment technologies for waste-water recycling—an overview. RSC Adv 2:6380–6388

Ho YS, McKay G (1999) Pseudo-second order model for sorption processes. Process Biochem 34:451–465

Jain AK, Gupta VK, Bhatnagar A, Suhas (2003) A comparative study of adsorbents prepared from industrial wastes for removal of dyes. Sep Sci Technol 38:463–481

Kiani GR, Sheikhloie H, Arsalani N (2011) Heavy metal ion removal from aqueous solutions by functionalized polyacrylonitrile. Desalination 269:266–270

Lagergren S (1898) About the theory of so-called adsorption of soluble substances. Vetenskapsakad Handl 24:1–39

Lakshmi UR, Srivastava V, Mall ID, Lataye DH (2009) Rice husk ash as an effective adsorbent: evaluation of adsorptive characteristics for Indigo Carmine dye. J Environ Manage 90:710–720

Li Q, Zhai J, Zhang W, Wang M, Zhou J (2007) Kinetic studies of adsorption of Pb(II), Cr(III) and Cu(II) from aqueous solution by sawdust and modified peanuthusk. J Hazard Mater 141:163–167

Luo T, Cui J, Hu S, Huang Y, Jing C (2010) Arsenic removal and recovery from copper smelting wastewater using TiO$_2$. Environ Sci Technol 44:9094–9098

Maturana AH, Perič IM, Rivas BL, Pooley SA (2011) Interaction of heavy metal ions with an ion exchange resin obtained from a natural polyelectrolyte. Polym Bull 67:669–676

Mittal A, Mittal J, Malviya A, Gupta VK (2009a) Adsorptive removal of hazardous anionic dye "Congo red" from wastewater using waste materials and recovery by desorption. J Colloid Interface Sci 340:16–26

Mittal A, Kaur D, Malviya A, Mittal J, Gupta VK (2009b) Adsorption studies on the removal of coloring agent phenol red from wastewater using waste materials as adsorbents. J Colloid Interface Sci 337:345–354

Mittal A, Mittal J, Malviya A, Gupta VK (2010a) Removal and recovery of Chrysoidine Y from aqueous solutions by waste materials. J Colloid Interface Sci 344:497–507

Mittal A, Mittal J, Malviya A, Kaur D, Gupta VK (2010b) Decoloration treatment of a hazardous triarylmethane dye, Light Green SF (Yellowish) by waste material adsorbents. J Colloid Interface Sci 342:518–527

Moreno-Piraján JC, Garcia-Cuello VS, Giraldo L (2011) The removal and kinetic study of Mn, Fe, Ni and Cu ions from wastewater onto activated carbon from coconut shells. Adsorption 17:505–514

Moscofian ASO, Pires CTGVMT, Vieira AP, Airoldi C (2012) Organofunctionalized magnesium phyllosilicates as mono- or bifunctional entities for industrial dyes removal. RSC Adv 2:3502–3511

Mungray AA, Kulkarni SV, Mungray AK (2012) Removal of heavy metals from wastewater using micellar enhanced ultrafiltration technique: a review. Cent Eur J Chem 10:27–46

Okasha AY, Ibrahim HG, Elatrash MS, Marie A (2012) Removal of cadmium from aqueous solutions using adsorption technique: kinetics and equilibrium. Int J Environ Bioenergy 1:105–118

Ozdemir G, Ceyhan N, Ozturk T, Akirmak F, Cosar T (2004) Biosorption of chromium(VI), cadmium(II) and copper(II) by Pantoea sp. TEM18. Chem Eng J 102:249–253

Plaziński W, Rudziński W, Plazińska A (2009) Theoretical models of sorption kinetics including a surface reaction mechanism: a review. Adv Colloid Interface Sci 152:2–13

Rangel-Mendez JR, Streat M (2002) Mercury and cadmium adsorption by conventional and modified granular activated carbon. Water Res 36:1244–1252

Ren Z, Zhang G, Chen JP (2011) Adsorptive removal of arsenic from water by an iron–zirconium binary oxide adsorbent. J Colloid Interface Sci 358:230–237

3626

Int. J. Environ. Sci. Technol. (2015) 12:3613–3626

Ru X, Meng R, Zhang J, Li X (2011) Application of high efficiency inorganic adsorbent bentonite on removal of Ni(II) from aqueous solutions. Bioinform Biomed Eng 5:1–4

Sadeghi S, Sheikhzadeh E (2009) Solid phase extraction using silica gel modified with murexide for preconcentration of uranium(VI) ions from water samples. J Hazard Mater 163:861–868

Salam MA, Burk RC (2010) Thermodynamics and kinetics studies of pentachlorophenol adsorption from aqueous solutions by multi-walled carbon nanotubes. Water Air Soil Pollut 210:101–111

Saleh A, Gupta VK (2011) Functionalization of tungsten oxide into MWCNT and its application for sunlight-induced degradation of rhodamine B. J Colloid Interface Sci 362:337–344

Saleh A, Gupta VK (2012a) Photo-catalyzed degradation of hazardous dye methyl orange by use of a composite catalyst consisting of multi-walled carbon nanotubes and titanium dioxide. J Colloid Interface Sci 371:101–106

Saleh A, Gupta VK (2012b) Column with CNT/magnesium oxide composite for lead(II) removal from water. Environ Sci Pollut Res 19:1224–1228

Saleh A, Agarwal S, Gupta VK (2011) Synthesis of MWCNT/MnO$_2$ and their application for simultaneous oxidation of arsenite and sorption of arsenate. Appl Catal B Environ 106:46–53

Saleh A, Gupta VK, Al-Saadi AA (2013) Adsorption of lead ions from aqueous solution using porous carbon derived from rubber tires: experimental and computational study. J Colloid Interface Sci 396:264–269

Saleh A, Al-Saadi AA, Gupta VK (2014) Carbonaceous adsorbent prepared from waste tires: experimental and computational evaluations of organic dye methyl orange. J Mol Liq 191:85–91

Sheela T, Nayaka YA (2012) Kinetics and thermodynamics of cadmium and lead ions adsorption on NiO nanoparticles. Chem Eng J 191:123–131

Souag R, Touaibia D, Benayada B, Boucenna A (2009) Adsorption of heavy metals (Cd, Zn and Pb) from water using keratin powder prepared from Algerien sheep hoofs. Eur J Sci Res 35:416–425

Srinivasa RK, Anand S, Venkateswarlu D (2010) Adsorption of cadmium(II) ions from aqueous solution by TectonaGrandis L.F. (teak leaves powder). BioResources 5:485–494

Wang X, Guo Y, Yang L, Han M, Zhao J, Cheng X (2012) Nanomaterials as sorbents to remove heavy metal ions in wastewater treatment. Environ Anal Toxicol 2:1–7

Weber WJ, Morris JC (1963) Kinetics of adsorption on carbon from solution. J Sanit Eng Div 89:31–60

Wu G, Wang Z, Wang J, He Ch (2007) Hierarchically imprinted organic–inorganic hybrid sorbent for selective separation of mercury ion from aqueous solution. Anal Chim Acta 582:304–310

Zhang Y, Li Q, Sun L, Tan R, Zhai J (2010) High efficient removal of mercury from aqueous solution by polyaniline/humic acid nanocomposite. J Hazard Mater 175:404–409

Zheng Y, Lim S, Chen JP (2009) Preparation and characterization of zirconium-based magnetic sorbent for arsenate removal. J Colloid Interface Sci 338:22–29